Computer-Aided Planning of Patellofemoral Joint OA Surgery: Developing Physical Models from Patient MRI

Zohara A. Cohen[1,2], Denise M. McCarthy[3], Hrvoje Roglic[1,2], Jack H. Henry[2], William G. Rodkey[4], J. Richard Steadman[4], Van C. Mow[1,2], and Gerard A. Ateshian[1,2]

[1] Department of Mechanical Engineering, Columbia University, 500 W 120th St, MC4703, New York, NY 10027

[2] Orthopaedic Research Laboratory, Department of Orthopaedic Surgery, Columbia-Presbyterian Medical Center, 630 West 168th St, BB1412, New York, NY 10032

[3] Department of Radiology, Columbia-Presbyterian Medical Center, Milstein Hospital Building, 3-248, New York, NY 10032

[4] Steadman-Hawkin Sports Medicine Foundation, 181 W. Meadow Drive, Suite 1000, Vail, CO 81657

Abstract. Generally, the surgical procedures employed in the treatment of patellofemoral joint (PFJ) osteoarthritis (OA) aim, either explicitly or implicitly, to alter the biomechanics of the osteoarthritic joint (i.e., improve motion and load transmission characteristics). Because of the mechanical nature of some of these surgical objectives, they can be evaluated prior to and subsequent to surgery by using an appropriate patient-specific physical model of the patient's PFJ, derived from 3D MRI data. This study describes the process by which such patient-specific physical models can be created using standard clinical imaging modalities.

Introduction

Currently, the clinical consensus is that the success of surgery for PFJ OA is highly variable and often unpredictable. Much of the data used in the decision making process derive from clinical examinations, supported by standard radiographic images that provide only indirect evidence of the severity of osteoarthritic damage in the diseased joint. The results of various procedures for the treatment of PFJ OA as well as patellar instability have been described in the literature for decades. The estimated success rate of patellofemoral PFJ surgery for osteoarthritis OA is 60%, excluding replacement arthroplasty. The long-term aim of this project is to improve this success rate by providing a new set of tools to help orthopaedic surgeons in planning their surgical treatment of PFJ OA.

One of the leading hypotheses for the initiation and progression of PFJ OA is that excessive stresses in the articular layers lead to degeneration by promoting a rate of tissue degradation that exceeds its rate of repair. From a clinical perspective, it is also believed that excessive articular contact stresses may contribute to the pain experienced by OA patients. Therefore, the premise of the current study is that successful planning of the outcome of PFJ OA surgery is dependent on a reliable prediction of changes in the articular contact area and stresses which would result from surgery. Because of the complexity of the articular topography of the PFJ, an accurate representation of the surfaces is required, which can be obtained from magnetic resonance imaging (MRI). Furthermore, such surgical planning is dependent on the ability to predict the forces which develop within the various structures of the joint, including articular contact forces, ligament forces, and other soft tissue interactions, that are dependent on the muscle forces acting across the joint. In this study, we describe our current progress on the development of physical models of patient knee joints from MRI, which can be used for the calculation of such parameters as contact areas, stresses and forces across the PFJ under various configurations of loading, as well as changes in these parameters following surgical simulations.

Computer-Aided Orthopaedic Surgery

Several investigators have used computer models to evaluate orthopaedic surgical procedures. Delp and co-workers developed a computer model [14,18] which they applied to investigate surgical treatments on the ankle [15,16], hip, and knee [17] joints, as well as gait [19]. Chao and co-workers applied a 2-D rigid-body-spring-model to evaluate wrist [3,27,31] and knee joint mechanics [9,32]. Furthermore, Chao and co-workers proposed methods to plan various surgeries for individual patients using their model [9] and created a computer software program to analyze knee osteotomy [8]. Other authors have also investigated the use of computer models to plan surgeries, mostly for the hip joint [7,37,38,39,40,51], but for the wrist [33] and tibia [48] as well. Finally, some investigators have reported use of guidance tools and robots in the operating room to aid the surgeons [35,39,41]. However, these studies generally have not focused on OA nor have they relied on such parameters as articular contact forces, areas and stresses. As a result, they have not attempted to reproduce the articular surfaces accurately. In this study, accurate topographic models of the patient's PFJ are developed from MRI data.

MRI of Articular Cartilage

Magnetic resonance imaging of articular cartilage has been the subject of intense research in recent years. Until recently, identification of cartilage defects could be made only by arthroscopy or surgery. Accurate, early, MR diagnosis can potentially tailor arthroscopy and surgery. The use of MR imaging has also been considered to show promise as a potential outcome measure for therapeutic studies by a task force of the Osteoarthritis Research Society [2]. The appearance of cartilage has been described on many MR sequences. T1- and T2-weighted spin echo images, which have both been advocated, are limited by a minimum practical slice thickness of 2-3 mm. Newer techniques include magnetization transfer and gradient echo imaging. Magnetization transfer techniques have been used to increase the contrast between cartilage and bone [50], however, magnetization transfer is not widely available and the subtraction method required introduces error.

Gradient echo imaging allows acquisition of thin contiguous slices in a volume which can be reformatted in multiple planes. Furthermore, gradient echo imaging has greater signal-to-noise in each slice than spin echo images [45]. In 1993, a study which compared T1-weighted, proton density, T2-weighted, spoiled GRASS, GRASS, and fat suppressed spoiled GRASS concluded spoiled GRASS best for cartilage [44]. Fat suppressed spoiled GRASS images were also more accurate than magnetization transfer in cartilage thickness determination of cadaver ankle articular cartilage [52]. High resolution volume spoiled GRASS cartilage sequences have been used in cadavers with 1-2 mm slice thickness to determine cartilage thickness in cadaver knees with precision [11-13,23]. In our own prior studies, we compared cadaver knee joint MRI measurements of cartilage topography and thickness against stereophotogrammetric measurements, and demonstrated sub-pixel accuracies (0.16 mm on average for topographic measurements, 0.32 mm on average for thickness measurements, on the patella and femur) [13].

Currently, for patient MRIs, we acquire two sets of images for each patient visit. The first set employs the cartilage-specific sequence proposed by Disler et al. and Peterfy et al. [20,21,42,43], which we have successfully implemented in our own studies [12,13]. This sequence consists of a 3-D volume spoiled GRASS with fat suppression, sagittal acquisition, TR=52 ms, TE=5 ms, flip angle=40°, field of view (FOV) = 12 to 16 cm (to enclose the entire articular layers of the knee), matrix = 256x160, 1 NEX, 60 contiguous 1.5 mm slices, with a duration of 8:56 minutes, and with the knee in full extension inside a linear extremity coil (Fig. 1a). The second set (Fig. 1b) consists of a sagittal acquisition, TR=550 ms, TE=15 ms, FOV = 16 cm, matrix = 256x192, slice thickness = 4 mm, acquisition time = 3:35 minutes, acquired in the body coil (50 cm diameter) at the maximum knee flexion angle permitted within the space constraints (typically, 50°-70° of flexion, 60° on average). The first set of images is used to get accurate anatomic measurements of the articular layers while the second set of images is used to determine the position of the patella relative to the femur, at a flexion angle where the PFJ contact force, contact area and contact stresses are close to their highest values.

Segmentation of MR images is performed using a custom-written semi-automated cubic B-spline snake procedure to extract the contours of the articular and sub-chondral bone surfaces (Fig. 2). This technique has been shown to achieve equal accuracy as manual segmentation in our previous cadaver study [13] while decreasing the time required for segmentation of all 60 slices by more than tenfold, down to approximately 2 hours.

Using the femoral and patellar bone contours from the two MRI sequences, a surface registration procedure is applied to realign the highly accurate cartilage surfaces acquired near full knee extension in the first sequence into the flexed position assumed by the patient in the second sequence. A surface proximity algorithm [5,47,49] is employed to determine the articular contact areas in the patient PFJ for the given flexed position (Fig. 3a). This articular contact area represents the baseline contact configuration which may serve for analyzing subsequent changes, either from post-surgical MRI or from surgical simulations performed on the physical model constructed from MRI data. Other information of significant value which can be obtained from the first MRI sequence is the thickness of the articular layer over the entire joint surface. Thickness maps can be used to track the changes in a patient's cartilage layer over time. A repeatability study performed on the knee of one volunteer over two sets of measurements showed a root-mean-square difference in thickness of 0.40mm, 0.27mm and 0.60 mm for the patella, femur and tibia respectively, precisions which compare favorably with the thickness measurement accuracy determined in the cadaver study [13]. Correlations may be found in some patients between regions of cartilage degeneration, as assessed from the thickness maps, and the location of the articular contact areas (Fig 5 a,c).

3D Multibody Modeling of the Patellofemoral Joint

Building on the work of previous investigators [6,24,25,28,29,30], we have recently developed a general interactive mathematical 3D model, capable of simulating different joints [34]. The model employs a quasi-static equilibrium analysis that predicts the equilibrium pose, contact areas, contact forces, and ligament forces of multiple bodies (bones and soft tissues) interacting together. Complex bone and articular surfaces are accurately represented by mathematical surfaces, and the contact stress between surfaces is approximated by various functions of the surface proximities. Ligaments are modeled as line segments whose forces are linearly or nonlinearly dependent on their length, stretch, or strain. Constant loads are applied through tendons to simulate muscle forces, and the tendons may loop through tendon pulleys connected to various bones. The model permits wrapping of the tendons and ligaments around bone and articular surfaces (e.g. the quadriceps tendon wrapping around the femoral trochlea) by imbedding particles in the ligaments and tendons, and letting these particle bodies interact with the surfaces. External forces and moments can be applied to any of the bodies, either in a body-fixed coordinate system or in a global coordinate system (e.g., to simulate gravitational forces). Finally, any of the translational or rotational degrees-of-freedom of a moving body may be optionally constrained (e.g., the knee flexion angle).

The Newton-Raphson iterative procedure was used to solve efficiently for the equilibrium condition; to expedite the calculations all components of the Jacobian matrix are evaluated analytically. The model was validated by reproducing results of actual cadaver knee joint experiments [34]. By using an analytical Jacobian formulation, the model converges very rapidly (2 to 10 seconds for most analyses). It provides graphical display of the results, and it allows the user to interactively change any of the input parameters.

In patient studies, a physical (multibody) model is constructed for the patient PFJ using the articular surface data, tendon and ligament insertions and bone contour data acquired from the first MRI sequence (Fig. 4,b and 5a ,b). The lines of action of the various quadriceps muscle components (vastus medialis obliqus, vastus lateralis, rectus femoris+vastus intermedius+vastus medialis longus can be inferred from manual segmentation of the muscle contours, and current work is in progress to assess the accuracy of this process. The muscle force magnitudes are adjusted so that the contact map generated from MRI is reproduced by the model. The properties of the soft tissue structures incorporated into the patient PFJ multibody model (articular cartilage, quadriceps tendon and patellar ligament stiffnesses) are currently obtained from the literature, since these properties cannot as yet be determined from MRI using current techniques.

Surgical Simulations

Many operations are available for the treatment of PFJ OA. These treatments may be divided into four categories:

1. Arthroscopic Procedures: lateral retinacular release, patellar shaving, lysis of adhesions, combinations.
2. Open Procedures: tibial tuberosity transfer (Hughston, Maquet, Elmslie-Trillat, Fulkerson), advancement of the VMO, lateral retinacular release, combinations.
3. Osteotomy: high tibial, distal femoral.
4. Resection: facetectomy, patellectomy.

However, not all patients respond to a given operation [1,26] and most of the surgical procedures relieve pain to a disappointingly variable degree. Therefore, in view of the numerous surgical procedures that have been used with variable success for the treatment of PFJ OA, there exists a significant need for aiding the orthopaedic surgeon in the planning of surgery by providing estimates of the potential outcome for each of these procedures, alone or in combinations. Such a mechanism ideally should provide a quantitative measure to allow proper assessment of each procedure. In this study, we propose to use such measures as PFJ articular contact areas, forces and stresses.

For the purpose of surgical simulations, many of the procedures described above require relatively minimal modifications to the physical multibody model of the joint, relative to the baseline patient-specific data. For example, tibial tuberosity transfer operations can be simulated by relocating the insertion points of the patellar ligament bundles on the tibia and adjusting the applied quadriceps forces to maintain the same flexion moment on the tibia (Fig. 4a,b). The patient shown in Fig 4 previously had a tibial tuberosity transfer, but complains of persistent knee pain. Reverse surgical simulation shows that the transfer procedure did in fact decrease the stress in the patient's knee. However, looking at the contact map of the current configuration, the contact is still positioned laterally on the patella, perhaps a source of her current pain. Lateral retinacular release may be performed by decreasing the force in the vastus lateralis (VL) component of the quadriceps force, while, similarly, adjusting other muscle forces to maintain a fixed moment about the knee (Fig. 5). On the femur of the patient represented by Fig 5 there is a focal lesion that coincides with the location of maximum contact stress for that knee. A simulated VL release shows that this patient may receive only limited benefit from such surgery, due to the limited amount of medial shift in contact area and the small decrease in contact stress (0.46 MPa to 0.43 MPa). Likewise, advancement of the vastus medialis obliquus can be simulated by relocating the insertion of this muscle component onto the patella. Osteotomies would require re-orienting the lines of action of the muscles and/or relocating the patellar ligament insertion. Other procedures involve more elaborate modifications such as changes to the solid model representation of the patella for resection procedures or patella shaving (Fig. 6) which can be performed with a solid modeler, or incorporation of additional soft-tissue structures for the simulation of adhesions [47].

The sophistication of the patient-specific multibody model of the PFJ can be increased by modeling more of the soft-tissue structures surrounding the joint, such as capsular tissues or the fat pad. The need for incorporating more details into the model should be based on experimental verification of the model's predictive ability in the simulation of various surgeries. Such experimental verifications are currently under way in a clinical setting involving the efforts of orthopedic surgeons, radiologists and engineers at four institutions across the United States.

Conclusion

Generally, the aims of surgical procedures employed in the treatment of PFJ OA are to alter the biomechanics of the osteoarthritic joint (i.e., improve motion and load transmission characteristics). For example, the explicitly stated goals of the Maquet or Fulkerson procedures have been to reduce the joint contact forces or stresses, to increase the size or to shift the location of the contact areas, to increase the moment arm of various tendons, or a combination thereof. Within the clinical setting, it is generally believed that reduction of PFJ contact forces and stresses, as well as re-establishment of normal joint kinematics, will decrease joint pain and improve the patient outcome. However, a direct correlation between such biomechanical variables and patient outcome has never been investigated. Because of the mechanical nature of some of these surgical objectives, they can be evaluated prior to and subsequent to surgery by using an appropriate patient-specific physical model of the patient's PFJ, derived from 3D MRI data. This paper has summarized some of the technical aspects of our current progress toward this objective.

Acknowlegement: This study was supported in part by the Steadman-Hawkins Sports Medicine Foundation.

References

1. Aglietti P, Buzzi R, De Biase P, Giro n F: Surgical treatment of recurrent dislocation of the patella. Clin Orthop 308 (1994) 8-17
2. Altman R, Brandt K, Hochberg M, Moskowitz R: Design and conduct of clinical trials in patients with osteoarthritis: recommendations from a task force of the Osteoarthritis Research Society. Osteoarthritis Cartilage 4 (1996) 217-243
3. An KN, Himeno S, Tsumura H, Kawai T, Caho E YS: Pressure distribution on articular surfaces: application to joint stability evaluation. J Biomech 23 (1990) 1013-1020
4. Ateshian GA, Soslowsky LJ, and Mow VC : Quantitation of articular surface topography and cartilage thickness in knee joints using stereophotogrammetry. J Biomech 24 (1991) 761-776
5. Ateshian GA, Kwak SD, Soslowsky LJ, M ow VC: A stereophotogrammetric method for determining in situ contact areas in diarthrodial joints, and a comparison with other methods. J Biomech 27 (1994) 111-124
6. Blankevoort L, Kuiper JH, Huiskes R, Grootenboer HJ: Articular contact in a three-dimensional model of the knee. J Biomech 24 (1991) 1019-1031
7. Burk DL Jr, Mears DC, Cooperstein LA, Herman GT, Udupa JK: Acetabular fractures: three-dimensional computed tomographic imaging and interactive surgical planning. J Comput Tomogr 10 (1986) 1-10
8. Chao EYS, Lynch JD, Vanderploeg MJ: Simulation and animation of musculoskeletal joint system. J Biomech Eng 115 (1993) 562-568
9. Chao EYS, Sim FH: Computer-aided preoperative planning in knee osteotomy. Iowa Orthop J 15 (1995) 4-18
10. Cohen ZA, Kwak SD, Ateshian GA, Blankevoort L, Henry JH, Grelsamer RP, Mow VC: The effect of tibial tuberosity transfer on the patellofemoral joint: A 3-D simulation. Adv Bioeng, ASME, BED 33 (1996) 387-388
11. Cohen ZA, McCarthy DM, Ateshian GA, Kwak SD, Peterfy CG, Alderson P, Grelsamer RP, Henry JH, Mow VC: In vivo and in vitro knee joint cartilage topography, thickness, and contact areas from MRI. Trans Orthop Res Soc 22 (1997) 625
12. Cohen ZA, McCarthy DM, Ateshian GA, Kwak SD, Peterfy CG, Alderson P, Grelsamer RP, Henry JH, Mow VC: Knee joint topography and contact areas: validation of measurements from MRI. Proc Bioeng, ASME, BED 35 (1997) 45-46
13. Cohen ZA, McCarthy DM, Kwak SD, Legrand P, Fogarasi F, Ciaccio EJ, Ateshian GA: Knee cartilage topography, thickness, and contact areas from MRI: In vitro calibration and in vivo measurements. Osteoarthritis Cart (in press)
14. Delp SL, Loan JP, Hoy MG, Zajac FE, Topp EL, Rosen JM: An interactive, graphics-based model of the lower extremity to study orthopaedic surgical procedures. IEEE Trans Biomed Eng 37 (1990) 757-767
15. Delp SL, Statler K, Carroll NC: Preserving plantar flexion strength after surgical treatment for contracture of the triceps surae: a computer simulation study. J Orthop Res 13 (1994) 96-104
16. Delp SL, Komattu AV, Wixson RL: Superior displacement of the hip in total joint replacement: effects of prosthetic neck length, neck-stem angle, and anteversion angle on the moment-generating capacity of the muscles. J Orthop Res 12 (1994) 860-870
17. Delp SL, Ringwelski DA, Carroll NC: Transfer of the rectus femoris: effects of transfer site on moment arms about the knee and hip. J Biomech 27 (1994) 1201-1211
18. Delp SL, Loan JP: A graphics-based software system to develop and analyze models of musculoskeletal structures. Comput Biol Med 25 (1995) 21-34

19. Delp SL, Arnold AS, Speers RA, Moore CA: Hamstrings and psoas lengths during normal and crouch gait: implications for muscle-tendon surgery. J Orthop Surg 14 (1996) 144-151
20. Disler DG, Peters TL, Muscoreil SJ, Rat ner LM, Wagle WA, Cousins JP, Rifkin MD: Fat-suppressed imaging of knee hyaline cartilage: technique optimization and comparison with conventional MR imaging. Am J Radiol 163 (1994) 887-892
21. Disler DG, McCauley TR, Wirth CR, Fuchs MD: Detection of knee hyaline cartilage defects using fat-suppressed three-dimensional spoiled gradient-echo MR imaging: comparison with standard MR imaging and correlation with arthroscopy. Am J Radiol 165 (1995) 377-382
22. Eckstein F, Sittek H, Milz S, Putz R, Reiser M: The morphology of articular cartilage assessed by magnetic resonance imaging (MRI): reproducibility and anatomical correlation. Surg Radiol Anat 16 (1994) 429-38
23. Eckstein F, Gavazzeni A, Sittek H, Ha ubner M, Losch A, Milz S, Englmeier KH, Schulte E, Putz R, Reiser M: Determination of knee joint cartilage thickness using three-dimensional magnetic resonance chondro-crassometry (3D MR-CCM). Magn Reson Med 36 (1996) 256-65
24. van Eijden, TMGJ, Kouwenhoven E, Verbur g J, Weijs WA: A mathematical model of the patellofemoral joint. J Biomech 19 (1986) 219-229
25. Essinger JR, Leyvraz PF, Heegard JH, Robertson DD: A mathematical model for the evaluation of the behaviour during flexion of condylar-type knee prostheses. J Biomech 22 (1989) 1229-1241
26. Fulkerson JP, Schutzer, SF: After failure of conservative treatment for painful patellofemoral malalignment: lateral release or realignment? Orthop Clin North Am 17 (1986) 283-288
27. Garcia-Elias M, An KN, Cooney WP, Linsc heid RL, Chao EY: Transverse stability of the carpus: an analytic study. J Orthop Res 7 (1989) 738-743
28. Garg A, Walker PS: Prediction of total kn ee motion using a three-dimensional computer-graphics model. J Biomech 23 (1990) 45-58
29. Heegaard J, Leyvraz PF, Curnier A, Ra kotomanana L, Huiskes R: The biomechanics of the human patella during passive knee flexion. J Biomech 28 (1995) 1265-1279
30. Hirokawa S: Three-dimensional mathema tical model analysis of the patellofemoral joint. J Biomech 24 (1991) 659-671
31. Horii E, Garcia-Elias M, An KN, Bishop A T, Cooney WP, Linscheid RL, Caho EYS: Effect on force transmission across the carpus in procedures used to treat Kienböck's disease. J Hand Surg 15A (1990) 393-400
32. Hsu RWW, Himeno S, Coventry MB, Chao EYS: Normal axial alignment of the lower extremity and load-bearing distribution at the knee. Clin Orthop 255 (1990) 215-227
33. Jupiter JB, Ruder J, Roth DA: Computer -generated bone models in the planning of osteotomy of multidirectional distal radius malunions. J Hand Surg 17A (1992) 406-415
34. Kwak SD, Ateshian GA, Blankevoort L, Ahm ad, CS, Gardner TR, Grelsamer RP, Henry JH, Mow VC: A general mathematical multibody model for diarthrodial joints: application and validation using the patellofemoral joint. Adv Bioeng, ASME, BED 33 (1996) 239-240
35. Matsen FA 3rd, Garbini JL, Sidles JA, P ratt B, Baumgarten D, Kaiura R: Robotic assistance in orthopaedic surgery. Clin Orthop 296 (1993) 178-186
36. Millis MB, Murphy SB: The use of comput ed tomographic reconstruction in planning osteotomies of the hip. Clin Orthop 274 (1992) 154-159

37. Murphy SB, Kijewski PK, Simon SR, Chand ler HP, Griffin PP, Reilly DT, Penenberg BL, Landy MM: Computer-aided simulation, analysis, and design in orthopedic surgery. Orthop Clin North Am 17 (1986) 637-649
38. Murphy SB, Kijewski PK, Millis MB, Hall JE, Simon SR, Chandler HP: The planning of orthopaedic reconstructive surgery using computer-aided simulation and design. Comput Med Imaging & Graph 12(1988) 33-45
39. Nolte LP, Zamorano LJ, Jiang Z, Wang Q, Langlotz F, Berlemann U: Image-guided insertion of transpedicular screws: a laboratory set-up. Spine 20:497-500 (1995)
40. O'Toole RV, Jaramaz B, DiGioia AM 3rd, Visnic CD, Reid RH: Biomechanics for preoperative planning and surgical simulations in orthopaedics. Comput Biol Med 25 (1995) 183-191
41. Paul H, Bargar WL, Mittlestadt B, Musits B, Taylor RH, Kanzanzides P, Zuhars J, Williamson B, Hanson W: Development of a surgical robot for cementless total hip arthroplasty. Clin Orthop 285 (1992) 57-66
42. Peterfy CG, van Dijke CF, Janzen DL, Gluer CG, Namba R, Majumdar S, Lang P, Genant HK: Quantification of articular articular cartilage in the knee with pulsed saturation transfer subtraction and fat-suppressed MR imaging: optimization and validation. Radiology 192 (1994) 485-491
43. Peterfy CG, Majumdar S, Lang P, van D ijke CF, Sack K, Genant HK: MR Imaging of the arthritic knee: improved discrimination of cartilage, synovium, and effusion with pulsed saturation transfer and fat-supressed T1-weighted sequences. Radiology 191 (1994) 413-419
44. Recht MP, Kramer J, Marcelis S, Pathria MN, Trudell D, Haghighi P, Sartoris DJ, Resnick D: Abnormalities of articular cartilage in the knee: analysis of available MR techniques. *Radiology* 187 (1993) 473-478
45. Recht MP, Resnick D: MR imaging of artic ular cartilage: current status and future directions. Am J Radiol 163 (1994) 283-290
46. Roglic H, Kwak SD, Henry JH, Ateshian G A, Rodkey W, Steadman JR, Mow VC: Adhesions of the patellar and quadriceps tendons: mathematical model simulation. Adv Bioeng, ASME, BED 36 (1997) 261-262
47. Ronsky J, van den Bogert A, Nigg B: In vivo quantification of human patellofemoral joint contact. Proc Can Soc Biomech 8 (1994) 82
48. Sangeorzan BJ, Sangeorzan BP, Hansen ST, Judd RP: Mathematically directed single-cut osteotomy for correction of tibial malunion. J Orthop Trauma 3 (1989) 267-275
49. Scherrer PK, Hillberry BM, Van Sickle DC: Determining the in vivo areas of contact in the canine shoulder. J Biomech Eng 101 (1979) 271-278
50. Seo GS, Aoki J, Moriya H, Karakida O, Sine S, Hikada H, Katsuyama T: Hyaline cartilage: in vivo and in vitro assessment with magnetization transfer imaging. Radiology 201 (1996) 525-530
51. Sutherland CJ, Bresina SJ, Gayou DE : Use of general purpose mechanical computer assisted engineering software in orthopaedic surgical planning: advantages and limitations. Comput Med Imaging Graph 18 (1994) 435-442
52. Tan TCF, Wilcox DM, Frank L, Shih C, Trude ll DJ, Sartoris DJ, Resnick D: MR imaging of articular cartilage in the ankle: comparison of available imaging sequences and methods of measurement in cadavers. Skeletal Radiol 25 (1996) 749-755

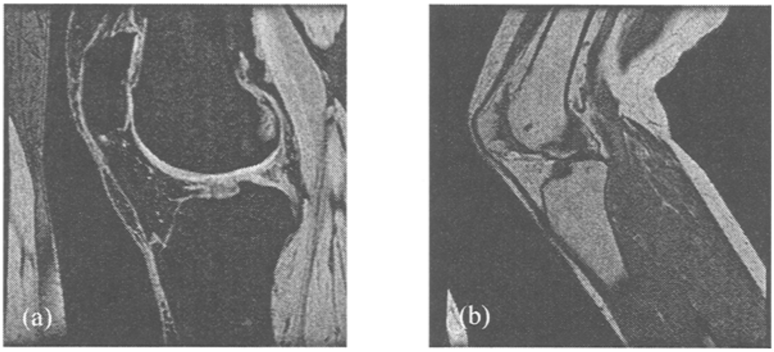

Fig. 1. Two image sequences are acquired for each patient: (a) a 9 minute cartilage sequence at full extension in a linear extremity coil and (b) a 4 minute sequence at 50°-70° of flexion in the full-body coil of the MRI scanner. This patient's patella exhibits arthritic lesions which can be visualized from the cartilage-specific sequence.

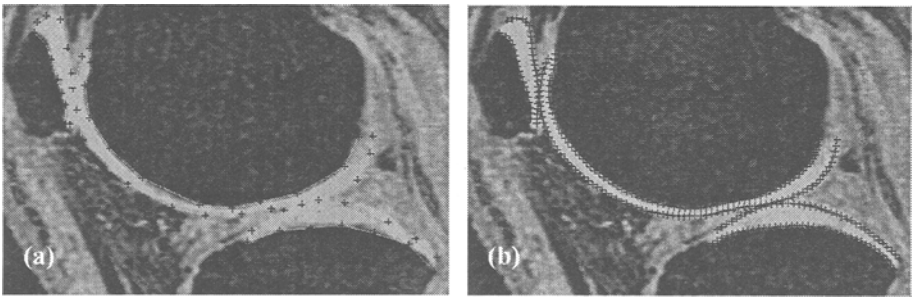

Fig. 2. Semi-automated segmentation of the cartilage layers from MRI: (a) A piecewise linear curve is first provided along the desired edge by manual digitizing (shown here for the cartilage and subchondral bone surfaces of the patella, femur and tibia). (b) A snake algorithm finds a best-fit cubic B-spline curve along the desired edges. The number of B-spline control points and knot spacing is determined from the initial curve [13].

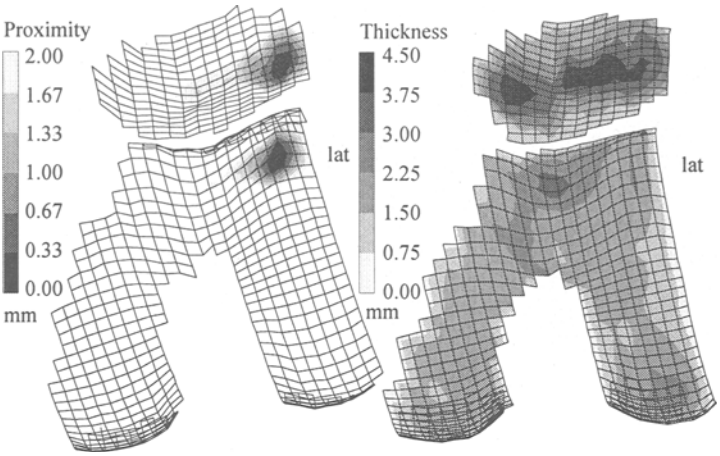

Fig. 3. Segmentation of patellar and femoral cartilage layers from patient MRI: (a) Contact map for patient with lateral subluxation at 70° flexion. (b) Cartilage thickness maps for same patient, showing a normal thickness distribution.

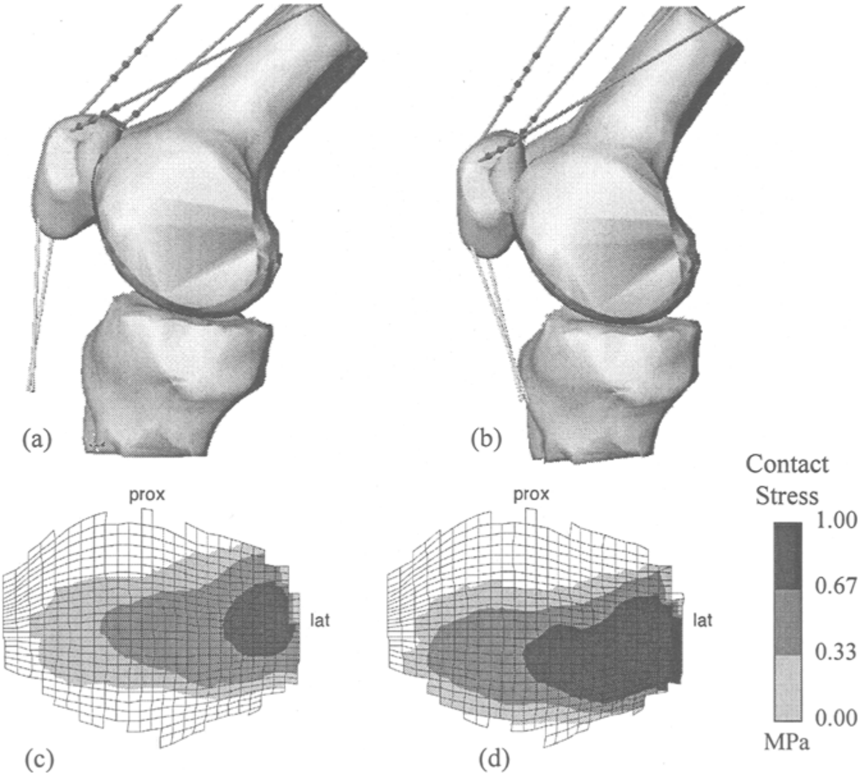

Fig. 4. Multibody model of the knee joint of a patient with previous tibial tuberosity elevation surgery. (a) Current configuration, (b) probable configuration before surgery (tuberosity shifted 15 mm posteriorly), (c) map of current stress distribution on the patella (avg. stress: 0.44 MPa) and (d) map of probable stress distribution before surgery (avg. stress: 0.57 MPa)

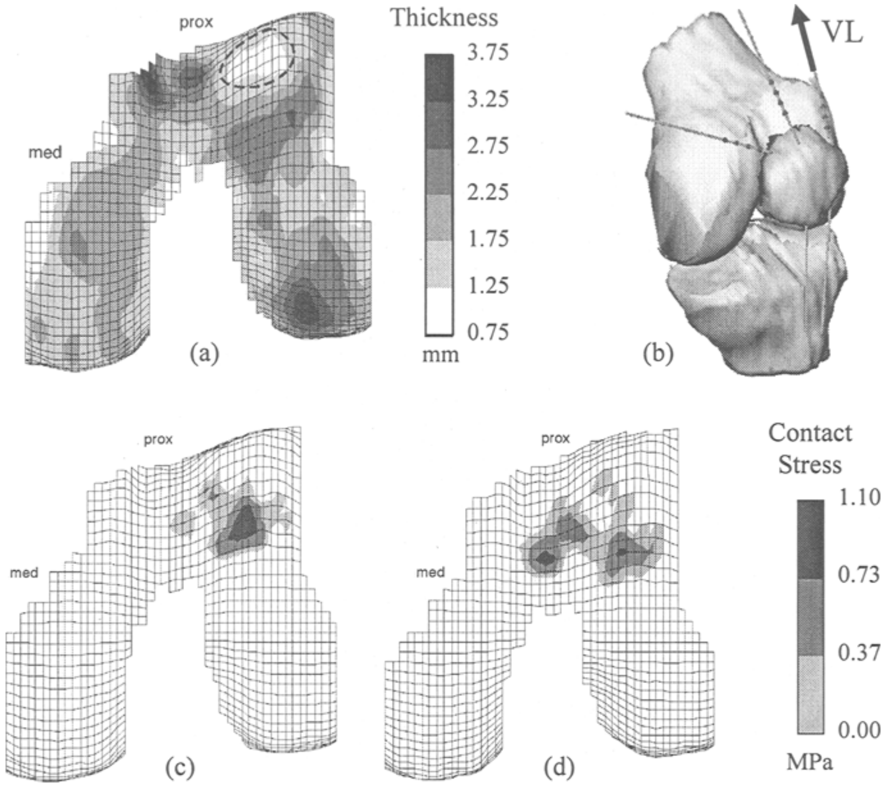

Fig. 5. Simulated VL release. (a) Cartilage thickness map for patient with lesion on lateral facet of trochlear groove (dashed curve), (b) computer model of same patient knee, (c) initial location of contact area on the femur (avg. stress: 0.46 MPa) and (d) contact pattern on femur after simulated VL release (avg. stress: 0.43 MPa)

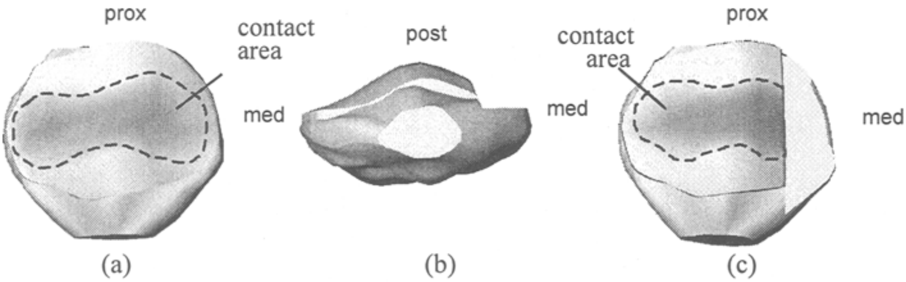

Fig. 6. Multibody analysis of facetectomy: (a) Pre-operative patellar geometry and contact areas; (b) resection of medial facet; (c) post-operative contact areas.